NANO LETTERS

2007
Vol. 7, No. 11
3266−3273

# Nanostructured Thin Films Made by Dewetting Method of Layer-By-Layer Assembly

**Bong Sup Shim,[†] Paul Podsiadlo,[†] Daniel G. Lilly,[†] Ashish Agarwal,[†] Jaebom Lee,[†,⊥] Zhiyong Tang,[†,⊗] Szushen Ho,[†] Pratima Ingle,[†] David Paterson,[†] Wei Lu,[§] and Nicholas A. Kotov*[,†,‡]**

*Department of Chemical Engineering, University of Michigan, Ann Arbor, Michigan 48109, Departments of Materials Science and Biomedical Engineering, University of Michigan, Ann Arbor, Michigan 48109, and Department of Electronic Engineering and Computer Science, University of Michigan, Ann Arbor, Michigan 48109*

*Received May 25, 2007; Revised Manuscript Received August 2, 2007*

**ABSTRACT**

**Layer-by-layer (LBL) assembly is one of the most ubiquitous coating techniques today. It also offers a pathway for multifunctional/multicomponent materials with molecular-scale control of stratified structures. However, technological applications of LBL are impeded by laborious and fluid-demanding nature of the process. While vertical organization of LBL films is natural for this technique, the control of lateral organization of the films is fairly difficult. Using the deposition of carbon nanotubes (SWNTs) and other nanoscale colloids, we introduce here a new approach to LBL based on dewetting phenomena, d-LBL. Its strengths include: (1) elimination of rinsing steps, (2) significant acceleration of the process, (3) improvement of lateral organization of LBL films, and (4) ability to produce nanostructured coatings from colloids when classical LBL fails. The generality of d-LBL can compete with traditional LBL and is demonstrated for cellulose nanowires, polyelectrolyte pairs, and semiconductor nanoparticles, metal oxides, and Au nanorods.**

Layer-by-layer (LBL) assembly is a simple and versatile method for material design with nanometer scale control over internal architecture, especially for the direction perpendicular to the substrate.[1−5] The technique has been already applied to a large variety of polymers and nanomaterials, such as polyelectrolytes, proteins, viruses, cells, nanoparticles, nanowires, nanotubes, etc., resulting in a palette of remarkable materials with stratified organization.[1−5] By analyzing the potential directions for further development of LBL and materials made by it, we can point out three fundamental issues that represent the bottlenecks of this technology:

1. Adsorption of some LBL multilayers can be time-consuming. Researchers have been actively looking for methods to accelerate the LBL process and techniques such as spraying,[6,7] spin-assisted LBL,[8−11] "electrically driven" LBL,[12] roll-to-roll process,[13] and "exponential" growth[14] had been discovered. However, acceleration of the buildup often comes at a price: some loss of structural control or universality.

2. In a typical LBL construct, each component must be adsorbed independently as a separate layer, followed by a rinsing step during which excess of the component is removed. Rinsing plays the key role in LBL assemblies because it results in precise nanoscale thickness control. However, the rinsing steps generate large amounts of waste, which is a deterrent for both practical applications, especially as a technique for nanomaterials production.

3. Besides the control of material organization in the direction perpendicular to the substrate, it is also important to provide means of structural control laterally to the substrate. This is particularly essential for LBL materials with "made-to-order" electrical, mechanical, and thermal transport properties that require organization of components in a scale of few nanometers.[15−17]

In this study, we want to suggest a potential resolution of these problems and a new approach to the LBL deposition.

In the past, we have shown that potential applications of LBL nanocomposites from axial structures such as single-walled nanotubes (SWNTs),[18] multi-walled nanotubes (MWNTs),[19] carbon fibers,[20] semiconducting nanowires,[21] and cellulose nanocrystals.[22] LBL assemblies of the carbon nanotubes are especially attractive as a basic example of the need of further LBL development. The unique, and in many cases superior properties achieved with LBL of carbon nano-

* Corresponding author. E-mail: kotov@umich.edu.
[†] Department of Chemical Engineering.
[‡] Departments of Materials Science and Biomedical Engineering.
[§] Department of Electronic Engineering and Computer Science.
[⊥] Current address: Department of Nanomedical Engineering, Pusan National University, Busan, 627-706, Korea.
[⊗] Current address: National Center for Nanoscience and Technology, Beijing 100080, China.

10.1021/nl071245d CCC: $37.00 
**Published on Web 10/13/2007**

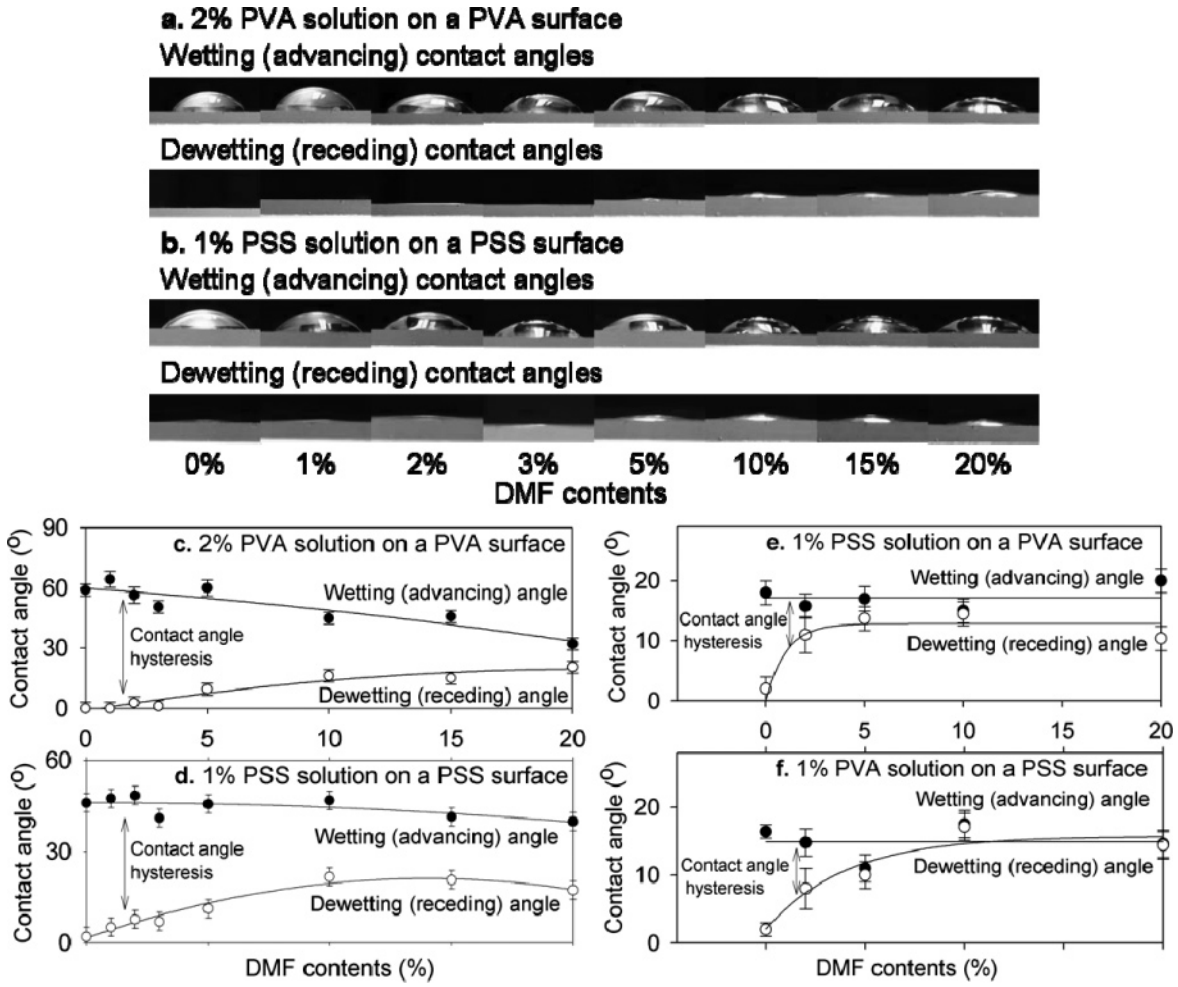


**Figure 1.** Contact angle measurements. (a) The advancing and receding droplets and (c) their contact angle of 2% PVA solution on a PVA coated surface. (b) The advancing and receding droplets and (d) their contact angle of 1% PSS solution on a PSS coated surface. Contact angle measurements of (e) 1% PSS solution on a PVA coated surface, and (f) 1% PVA solution on a PSS surface. There were dramatic changes in contact angle hysteresis or wetting angles between (c−d) and (e−f). Instant droplet spreading occurs in (e,f) because there are effective attracting forces between two different LBL polymers, the driving forces for LBL assemblies. However, dewetting(receding) angles in all cases were not different much because those attraction forces of advancing droplets in (e,f) no longer exist or significantly weaken by already formed LBL polymer adsorption so that the interactions involved in all receding droplets are the same kind polymer interactions as in (c,d).

tubes, the challenges of their production,[18,19,23−29] as well as their prospects for novel electronic and structural materials determined the choice of the primary model system for this study.

Here, we show that the LBL cycle can be drastically accelerated by eliminating the rinsing operations. Importantly, it can be done without sacrificing other attractive features of LBL multilayers, such as simplicity, universality, and stratification of the coatings. The LBL approach (d-LBL) described here takes advantage of the dewetting effect,[30,31] which occurs at solid−liquid interfaces for which the contact angle is high. This was achieved by adding small amount of dimethylformamide (DMF) to both polyelectrolyte and SWNT dipping solutions (see Supporting Information for the theoretical background of DMF addition). d-LBL shortens time for the preparation of macro-scale films by ∼30 times. It also produces quite unusual fishnet lateral morphology of the SWNT multilayers with fractal features, which resulted in improvement of the mechanical properties compared to all the previous reports.[18] Additionally, unique combination of d-LBL forces acting at the triple air−solid−liquid interface enables efficient alignment of the adsorbed axial species. Furthermore, d-LBL enables successful deposition of the coatings from branched $SnO_2$ nanowires, which failed with conventional LBL. Because of the 3D nature of these wires, it opens interesting possibilities for materials design. We also demonstrate that d-LBL is quite general and can be applied to other LBL materials such as Au nanorods (NRs), cellulose nanowires, polylectrolytes, and semiconducting CdTe nanoparticles (NPs). In the case of Au NRs, markedly different optical properties of d-LBL and regular LBL were obtained. So, overall, the d-LBL deposition can be an essential tool that can be useful to both accelerate and organize the multilayers for a wide array of nanoscale systems with optional lateral dewetting pattern capability.[32,33]

**Results and Discussion.** Typical LBL assemblies consist of a series of four basic steps: (1) immersion of the substrate into solution of a polymer or other high molecular weight material, (2) rinsing to remove excess of the first component on a substrate, (3) immersion into a solution of a different

high molecular weight material, and (4) rinsing to remove excess of the second LBL component. The adsorption step of each component can take anywhere between few seconds to hours, while rinsing steps can take between few seconds and 10 min. These basic steps are then repeated as many times as necessary to reach a desired thickness of the film. Now let us consider the case when the LBL solutions are dewetted from the substrate surface. Such solutions are not supposed to leave an appreciable amount of fluid on the surface because this is not thermodynamically and kinetically favorable. If the cases of extreme wetability and hydrophobicity are avoided,[34−36] rinsing steps can be completely eliminated and the LBL deposition in a cycle may be reduced to only two steps. The questions now is "*Is it possible?*" If yes, can one achieve the deposition of the multilayers in the cyclic manner similar to what we typically have in case of LBL? Are the properties of the produced material comparable to those made by conventional LBL?"

Single-walled carbon nanotubes (SWNTs) dispersed in poly(styrene sulfonate) (PSS) demonstrated successful LBL assembly with polyvinyl alcohol (PVA).[37] The adsorption steps of nanotubes in our experience tend to require substantially longer time than that for a polymer. One can speculate that this is because of the lower charge density and/or greater rigidity of the carbon nanotube, which in turn, results in the sluggishness of molecular and nanoscale rearrangements necessary for the successful adsorption.[38] To realize dewetting conditions, we added DMF to solutions of both SWNT−PSS and PVA. Advancing (wetting) contact angles and receding (dewetting) contact angles were measured for different DMF concentrations in PVA and PSS solutions (Figure 1). As DMF is added, wetting states of solutions over a surface dramatically change from stable to unstable which yields a substantial increase of receding contact angles (Figure 1). The latter are particularly important for d-LBL from the perspective of removal of the excess of the solution, brought about by pinning of the droplets with low contact angles. Note the broad maximum in receding angle indicating existence of optimal DMF contents. Advancing contact angle is convenient for evaluation of attractive forces between the polymers in a solution and on the surface. It decreases as the attraction becomes stronger. So, the advancing contact angles between different polymers in solution and on substrate, i.e., pairs such as PVA (solution) + PSS (solid) or vice versa, are quite small regardless of DMF contents (Figure 1e,f), which is beneficial for LBL adsorption. Simultaneously, advancing angles between same polymers, i.e., pairs such as PVA (solution) + PVA (solid) and PSS (solution) + PSS (solid), are very high (Figure 1c,d). Altogether, it is consistent with the picture of intermolecular forces necessary for layer alternation in d-LBL and demonstrates that the balanced increase of surface tension may be achieved in this system.

Now, let us demonstrate that dewetting (a) results in self-cleansing on the topmost LBL surface (Figure 2) and (b) does not prevent LBL growth. SWNTs are quite convenient for characterizing the efficiency of self-cleansing by dewetting because they provide distinct micro-/nanoscale topological features. So, the cyclic d-LBL procedure was performed as described in the Experimental Section, alternating deposition and dewetting of a substrate with solutions of PVA and SWNT−PSS both in 10% DMF/water mixture. The total adsorption time of SWNTs was reduced from 10 min to 10 s. The surface morphology of d-LBL films as observed by SEM (Figure 2) is very similar to that of conventional LBL. There are no big aggregates of the coagulated components that should have formed when considerable quantities of solutions were left on the substrate. Note, however, that there are microscopic islands generated by receding liquid[39,40] (Figure 2d, SEM, marked by arrows). They are quite rare and fairly small; their overall effect on the film structure is limited mainly to adsorption curves (see below). No streaks or other large-scale nonuniformities produced by moving meniscus were observed (Figure 2g−l).

To examine efficiency of the d-LBL technique, we compared the d-LBL and conventional LBL side-by-side using UV−vis absorbance. The optical density trends in d-LBL display generally larger increments and the overall trend has a pronounced upward swing, while conventional LBL displayed a typical linear growth (Figure 3 a). The curve characterizing the overall accumulation of the material in d-LBL appears to be exponential, which further accelerated the growth in addition to the reduced number of steps. The linear absorbance trend was recovered when rinsing was reintroduced, for instance, during the stage of PVA adsorption (Figure 3b). Thickness trends of the two LBL assemblies, $[\text{PVA dewet/SWNT dewet}]_n$ and $[\text{PVA rinse/SWNT rinse}]_n$, were also compared by ellipsometry measurements (Figure 3a). Against expectations, the thickness increments in the ellipsometry results are clearly linear. A probable explanation of the discrepancies between exponential trend in UV−vis and linear tend in ellipsometry is that small nano- to microscale islands seen in SEM (Figure 2). They are likely to completely absorb light of a He−Ne laser or Xe lamp used in UV−vis spectrophotometer. Because ellipsometric measurements are based on reflected beam, the islands are not accounted for in ellipsometric thickness, which reflect mostly linear accumulations of the material in the dominant surfaces of the films. UV−vis data contain the contribution of the islands and display the cumulative accumulation of the material, and hence, with the upswing.

The efficiency of d-LBL in comparison to conventional LBL can be calculated from processing time of the films and taking into account difference in growth increments. The comparison is done for the following two settings: (1) d-LBL [PVA (10 s) dewet (30 s)/SWNT (10 s) dewet (30 s)] and (2) conventional LBL [PVA (10 min) + rinse (1 min)/SWNT (10 min) + rinse (1 min)]. For d-LBL, the cycle length is ∼80 s, while for conventional LBL, it is 1320 s. Because the ratio of slopes for the two optical density regressions (Figure 3a,b) is 1.81, d-LBL is at least ∼30 times more efficient as applied to SWNT than conventional LBL in timewise comparison with similar film qualities when considered total dewetting finished within much less than 30 s.

Interestingly enough, when one simply repeats the dewetting adsorption step with the same solution without

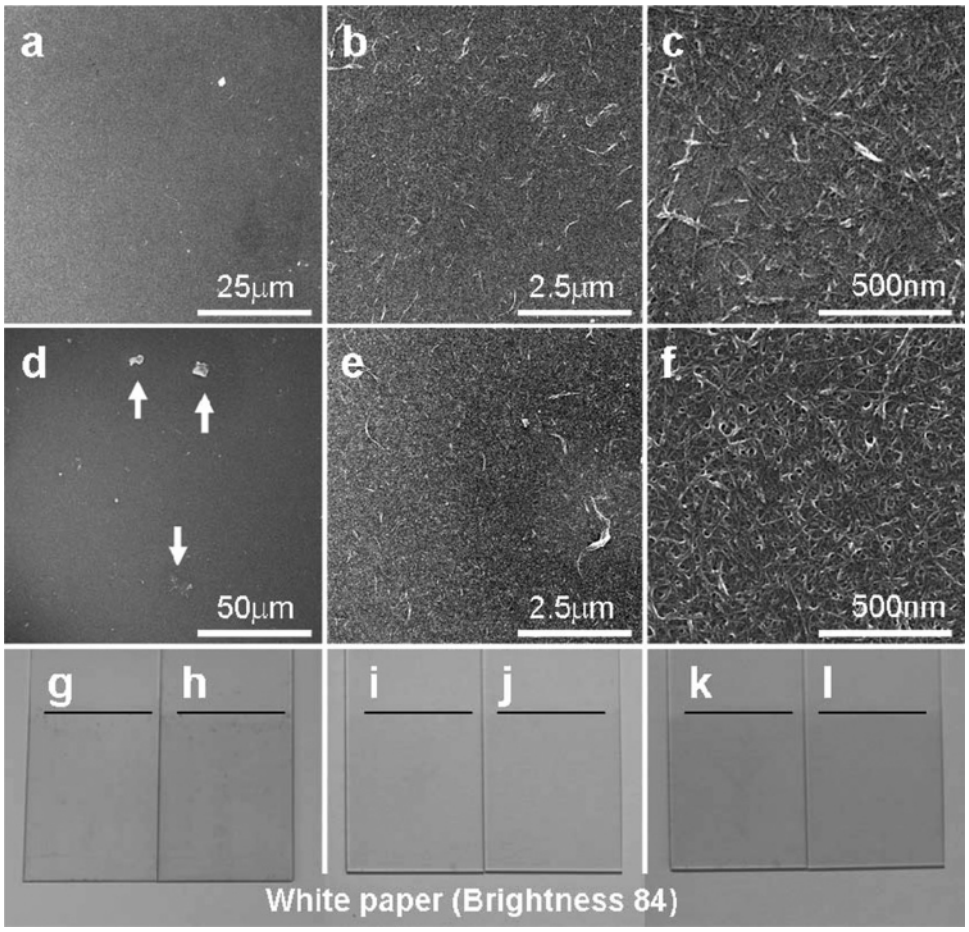


**Figure 2.** Comparative evaluation of basic properties of films made by dewetting and classical LBL. SEM images with different magnification of (a−c) conventional LBL ([PVA (10 min) rinse/SWNT (10 min) rinse]$_5$, (d−f) d-LBL ([PVA (10 s) dewet/SWNT (10 s) dewet]$_5$. The arrows in (d) indicate typical islands caused by dewetting instability. (g,h) Optical appearances of d−LBL coated films, ([PVA (10 s) dewet/SWNT (10 s) dewet]$_n$. (g) $n = 2$ and (h) $n = 3$. (i) [PVA (10 s) dewet + rinse/SWNT (10 s) dewet]$_2$, (j) [PVA (10 min) rinse/SWNT (10 min) rinse]$_2$, (k) [PVA (10 s) dewet + rinse/SWNT (10 s) dewet]$_3$, (l) [PVA (10 min) rinse/SWNT (10 min) rinse]$_3$. For all the images, the very top layer was SWNTs.

intermediate adsorption of the other component, for instance, a series of SWNT dewetting adsorption, a greater amount of this component is accumulated on the surface (Figure 3b). The UV−vis data can also be confirmed by AFM (Figure 3c−e). This result is quite useful when one needs to increase the relative content of one of the components. In the case of SWNTs, it can be used to control the nanotube loading without increasing their linear charge density, which is always connected to the greater damage of the conjugated $\pi$-orbital system or thicker polymer coating around the graphene stem.[41]

As one can notice, adsorption steps take substantially less time in d-LBL. High-density layers can be obtained substantially more quickly than in conventional LBL. The slope of the material accumulation curves even in linear representation is also greater (Figure 3). Elimination of rinsing steps, and thus, the inevitable desorption of a portion of adsorbed layer, is a simple but probably an incomplete answer here because the material accumulation curves have higher slopes even when one rinsing step is used. Additionally, the time of each d-LBL cycle for SWNT is so much shorter that it must be included in consideration. Within the limit of existing knowledge of transfer during dewetting, this observation can be explained by acceleration of the mass transport due to vigorous convection flows in the vicinity of the interface during the dewetting movements. Furthermore, metastable adsorbed components are readily stabilized by instant exposure to air after dewetting. Overall, dewetting eliminates the bottleneck of diffusion limiting kinetics, which is a source of process acceleration in spray deposition,[6,7] spin-LBL,[8−11] and electro-LBL.[12] Therefore, the synergic combination of flow-induced material transport and instant adsorption stabilization dramatically facilitated the adsorption reactions but without any external devices.

The d-LBL was further applied to fabrication of a free-standing SWNT−polymer composite film. The 300-layered d-LBL assemblies, [PVA dewet + rinse/SWNT dewet]$_{300}$, resulted in about $\sim$2 $\mu$m thick film (Figure 4) and displayed $229 \pm 36$ MPa in tensile strength and $0.08 \pm 0.014$ in strain. These mechanical properties are substantially better than those of SWNT-based composite films constructed by conventional LBL assembly in several previous studies,[18,19] which indicates that the dewetting process can not only accelerate the LBL procedure but also produce better materials.

When SWNTs are adsorbed on a PVA layer, d-LBL gives an unusual 2D film morphology of the films, which can be

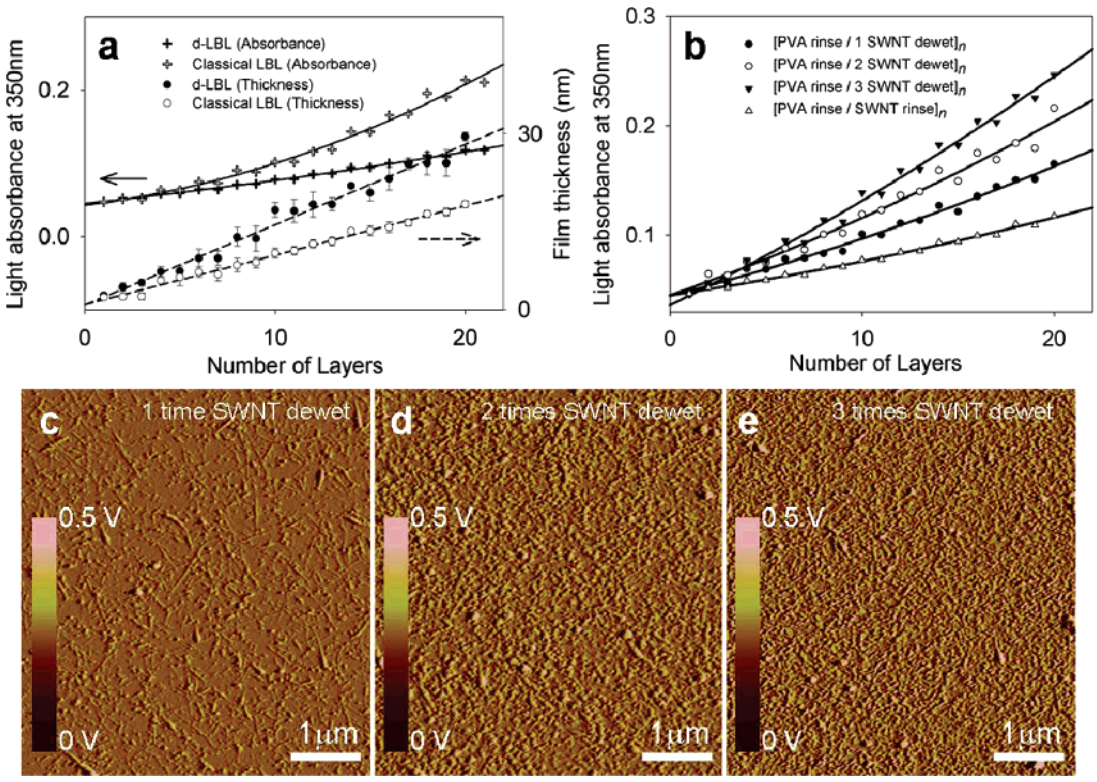


**Figure 3.** Adsorption trends of dewetting and classical LBL. (a) Comparison of UV−vis accumulation curves for absorbance at 350 nm and ellipsometry thickness measurements of d-LBL without rinsing and classical LBL of $[PVA/SWNT]_n$ system. (b) Accumulation curves for multiple dewetting procedure, [PVA (10 s) dewet + rinse/$x$ times SWNT dewet]$_n$, ($x$ = 1, 2, 3), and [PVA (10 min) rinse/SWNT (10 min) rinse]$_n$. AFM images when SWNT deposition was repeated 1 **(c),** 2 (d), and 3 (e) times in a row.

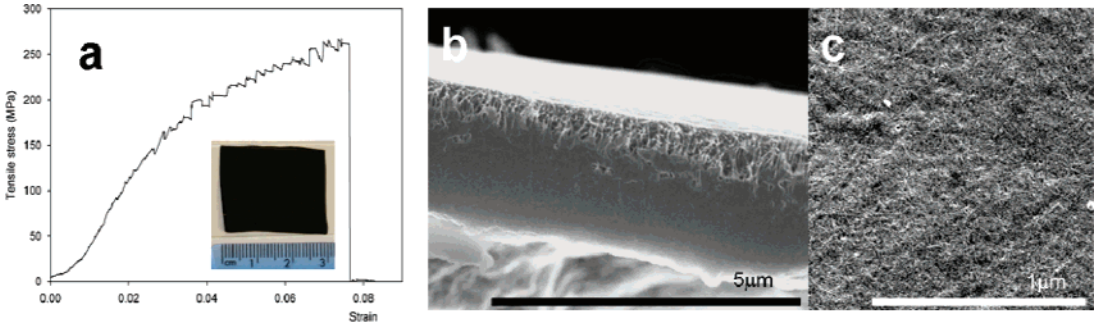


**Figure 4.** Mechanical testing of a SWNT film fabricated by d-LBL. (a) 300 layer d-LBL film, [PVA dewet + rinse/SWNT dewet]$_{300}$, was fabricated and tested in mechanical strength. Stress−strain curve of the d-LBL free-standing film and photoimage (insert). (b) Cross-sectional and (c) plane view SEM images of the SWNT−polymer composite film fabricated by d-LBL technique. Densely packed and finely distributed SWNTs make interwoven structures.

described as the network structures[42] (Figure 5). The fractal networks can be exceptionally interesting for charge transport and mechanical properties (Figure 4). Their extensive interconnectivity is essential in many nanotube applications such as fuel cell membranes and flexible electronics.[48] The fractal patterns emerge because of the dewetting movements of a three-phase meniscus. They originate from the two different sets of forces exerting on SWNTs: the dewetting forces that trigger the unsteady and unstable movement of fluid along adsorbed SWNTs, and the hydrodynamic forces caused by microflows close to the substrate surface. The actual pattern is a result of SWNT adsorption during the movements combined with restructuring the film[39,40,43] by surface tension at the triple interface.

The dynamics of dewetting can also be used to affect a different lateral organization. When one induces a unidirectional movement of the pool of 0.5% PSS/ 0.05% SWNT on the surface of the substrate by a gentle stream of air or simply by the effect of gravity, SWNT fibers show tendency to align as in previous study.[37] In this way, we increase the hydrodynamic component, which dominates the other forces. Alignments of nanotubes and other axial structures are quite important for a variety of functional properties of the nanostructured materials that include mechanical properties, charge transport, and thermal conductance. We want to point out that the concentration, receding/advancing contact angles, and the speed of the fluid movement in these systems are the key structural factors determining the lateral organization

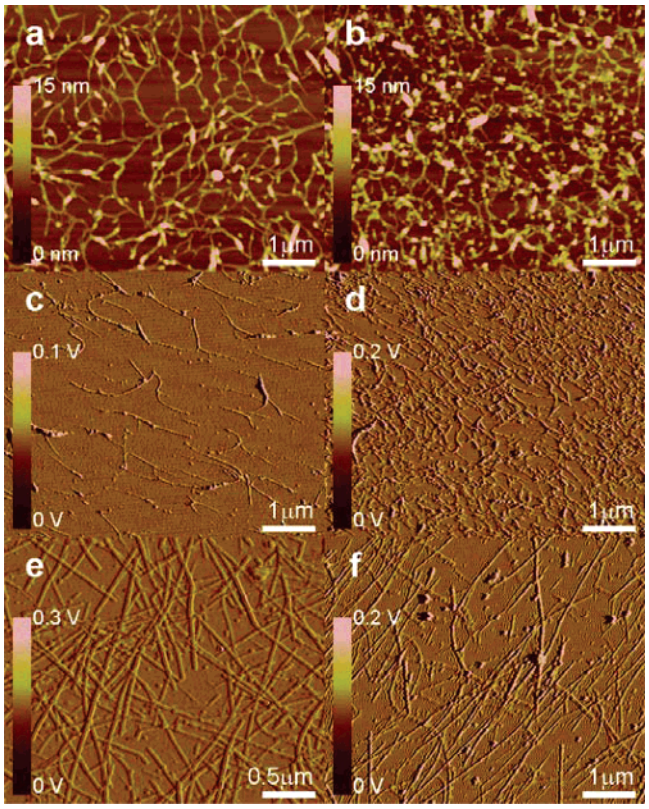


**Figure 5.** Lateral patterns by d-LBL. AFM images of (a) 1 bilayer and (b) 2 bilayers of [PVA rinse/SWNTs dewet] by dewetting forces dominating LBL mode, (c) 1 bilayer and (d) 2 bilayers of [PVA rinse/SWNT dewet] by hydrodynamic force controlled dewetting mode, and (e) 1 bilayer of [PVA rinse/cellulose NWs dewet] by dewetting forces dominating LBL mode and (f) 1 bilayer of [PVA rinse/cellulose NWs dewet] by hydrodynamic force controlled dewetting mode.

of the films in d-LBL. The presented two patterns are likely to be just some examples of potentially many patterns that can exist here brought about by the competition of forces during dewetting movements and other processes.[44]

This control of morphology is necessary for any axial nanocolloids rather than being limited only to SWNTs. Alignment of cellulose NWs in Figure 5f shows the generality of the morphology control by d-LBL. Obtaining aligned structures is essential for all rod- and wirelike building blocks. More complex packing motifs, such as fractal layers, are a function of not only geometry but also the properties of nanocolloids, for instance, their mechanical compliance with the flow, surface tension, and adhesion to the substrate, which will further increase the variety of potential in-plane morphologies of LBL layers.

It is necessary to show that d-LBL is applicable to the common basic components used for preparation of nanostructured thin films. As such, d-LBL of [poly(diallyldimethylammonium chloride), (PDDA) dewet/PSS dewet] and [poly(ethylenimine), (PEI) dewet/CdTe dewet] assemblies were performed (Figure 6). The consistent exponential growth trends both in UV−vis absorbance and ellispometry thickness in the [PDDA dewet/PSS dewet] d-LBL were observed. No micrometer-scale islands were observed. Instead, we saw somewhat increased roughness. In the case of another standard buiding block, such nanoparticles, d-LBL of [PEI dewet/CdTe dewet]$_n$ multilayers, displayed low-level exponential rise in UV−vis absorbance. These observations are consistent with those for SWNTs. Overall, the key LBL characteristics, such as complete surface coverage and molecularly fine structural controls, can be attributed to d-LBL as much as to the classical LBL.

Au nanorods (NRs) represent another fundamental building block in nanostructured thin films. Multilayers of Au NRs can also be easily made by d-LBL (Figure 6i−k). Importantly, d-LBL multilayer Au NRs display a qualitative distinction compared to the classical LBL. Greater efficiency of deposition results in denser layers with very strong mutual coupling of electronic oscillations in Au NRs absent in similar films made by classical LBL. Coupling of optical resonances in Au NRs is considered to be a prerequisite for engineering of materials with negative refractive index.

Another interesting example of d-LBL is the assembly of 20−50 nm $SnO_2$ nanowires that have 3-dimensional branched shapes with "thorns" of 1−2 $\mu$m in length (Figure 6g−h). These $SnO_2$ nanowires cannot be assembled by conventional LBL at all because of (1) limited surface charge (5mV) and (2) unfavorably small contact area to the adsorption surface due to branching. Oppositely, d-LBL produces films with stable growth with uniform adsorption increment from one cycle to the next.

**Conclusion.** A new LBL approach based on dewetting phenomena was introduced in this paper. It is efficient, economical, and fast. The scientific and engineering novelty also includes simplification of the procedure, decreased amounts of waste, and realization of the deposition for species when normal LBL fails (Figure 6g−k). It can also be used for creation of unique adsorption topographies, including fractal networks and aligned fibers. The experiments demonstrate that it is expected to be applicable to most existing LBL assembly systems and can potentially lead to nanostructured thin films with improved structural characteristics, mechanical, electrical, and optical properties.

**Experimental Section.** *Preparation of LBL Solutions.* The stable dispersion of SWNTs (Carbon Nanotechnologies, Inc.) with PSS (Sigma-Aldrich, MW 1 000 000) was prepared in an ultrasonic bath (VWR model 150HT) for 2 days. In a SWNT dispersion solution, PSS was varied from 0.5% to 2%, and SWNT concentration was adjusted to ~0.05% (= 0.5 mg/mL). PVA (Sigma-Aldrich, MW 70 000), PDDA (Sigma-Aldrich, MW 400 000), PEI (Sigma-Aldrich, MW 25 000), and PSS solutions were prepared with 0.5%, 1%, 2%, respectively. Preparation of CdTe semiconducting nanoparticles followed our previous article.[45−47] The $SnO_2$ nanowires were provided by Prof. Wei Lu.

*Film Characterization.* The contact angle measurements were performed on a polymer-coated surface that was prepared by LBL assembly technique. We dropped 20 $\mu$L PVA and PSS solutions to measure advancing contact angles and sucked back a few $\mu$L again to observe dewetting contact angles on a PVA and PSS surface, respectively. We repeated those measurements by varying contents of DMF in solutions.

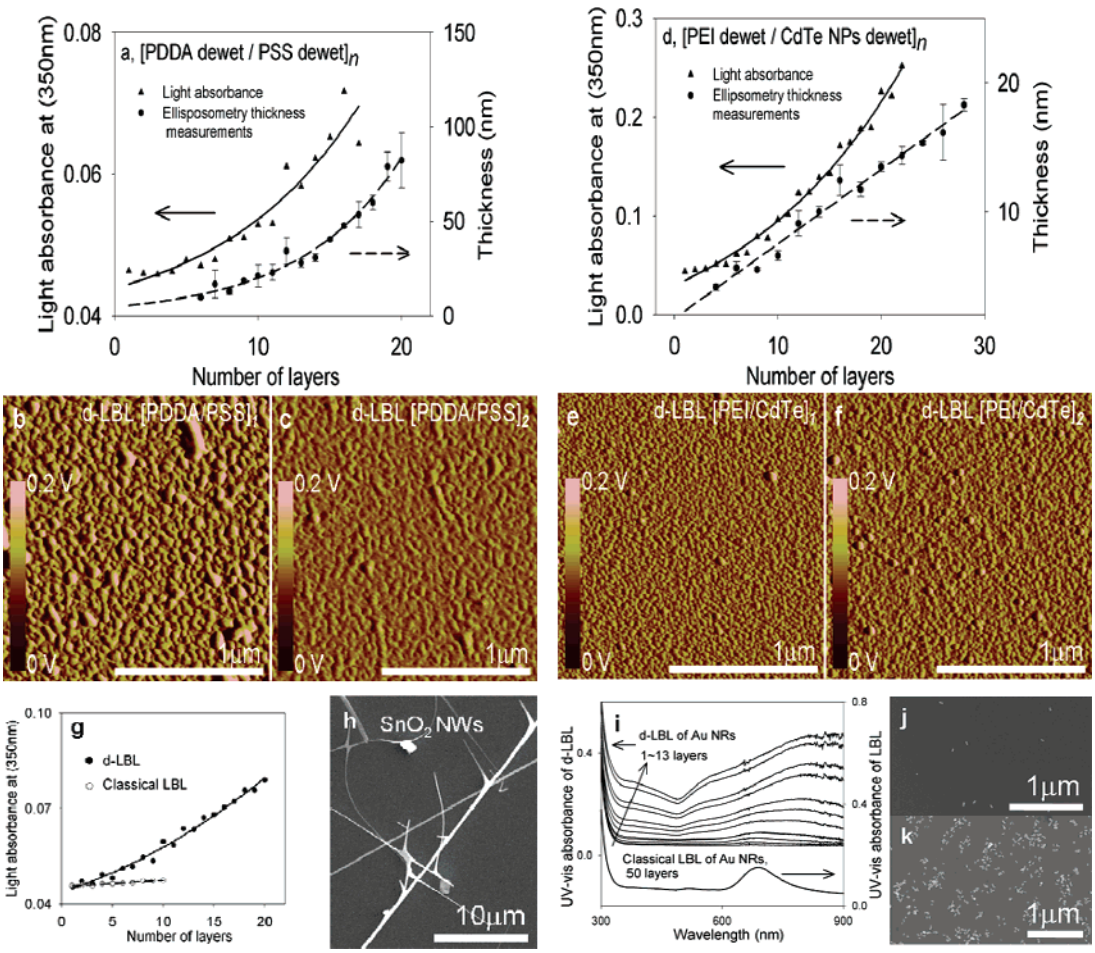


**Figure 6.** Applicability of d-LBL to typical nanoscale collods and polymers. (a−c) UV−vis, ellipsometry trends, and AFM film topology (1 and 2 layers) for d-LBL of solely polyelectrolyte layers [PDDA dewet/PSS dewet ]$_n$. (d−f) UV−vis, ellipsometry trends, and AFM film topology (1 and 2 layers) for d-LBL of nanoparticles [PEI dewet/CdTe dewet]$_n$. (g−i) Comparison of UV−vis trends in d-LBL and classical LBL for branched $SnO_2$ nanowires [$SnO_2$ dewet/PDDA/PAA]$_n$ (●) and [$SnO_2$/PDDA/PAA]$_n$ (○). No classical LBL deposition is observed. (h) SEM images of $SnO_2$ branched wires. (i) Comparison of UV−vis trends in d-LBL and classical LBL for Au NRs [Au NRs dewet/PVA]$_n$ and [Au NRs/PVA]$_n$. Note drastically different UV spectra. (i,k) SEM images of (j) [Au NRs rinse/PVA]$_2$, (k) [Au NRs dewet/PVA]$_7$.

The d-LBL samples for imaging were prepared on both Si substrates and glass slides depending on the measurement requirements. For d-LBL (polymer dewet), a glass slide was dipped in the polymer solution for 10 s and cleansed as dewetting modes. The last drops on the edges were removed by approaching Kimwipes. Normally, dewetting mode cleansing took less than 30 s, although these varied by contents of DMF, temperature and so on. All the conventional LBL or (polymer rinse) samples were done with 10 min dipping followed by rinsing in clean water for 1 min.

UV−vis spectroscopy (Agilent 8453) was performed on the samples of a glass slide. SEM (FEI, Nova Nanolab Dualbeam FIB and scanning electron microscope) and AFM (Digital Instruments, Nanoscope 3a) were used to observe the samples prepared on a Si substrate. The ellipsometry (J. A. Woollam M-44) measurements were collected three times with varying measurement directions of the samples on a Si substrate and then the values were averaged. To determine the thickness increment trend is linear, not exponential as in the Figure 3a, the $R^2$ values were calculated to be 0.9819 for linear and 0.9036 for exponential regressions.

Adsorption morphology patterning experiments were performed in varying the position of a substrate during dewetting movements or blowing mild air. In dewetting force dominating pattern experiments, the substrate was held in a horizontal plane (Figure 5a,b). Alignments of SWNTs were performed by holding the substrate in vertical position to use the gravity force to speed up dewetting movements (Figure 5c,d), and alignments of cellulose NW were done by using mild air blow to guide dewetting lines (Figure 5f).

Mechanical stretching test results of the 300 layered d-LBL film were obtained by testing three times (100Q model, TestResources Inc.) after the film was peeled off from the glass substrate by dipping in 1% HF solution.

For the demonstration of generalized d-LBL assemblies, i.e., [PDDA dewet/PSS dewet] and [PEI dewet/CdTe dewet], 0.5% polymer solutions were used and 10% DMF were added. d-LBL procedures are following: 10 s dipping and less than 30 s of self-cleansing by dewetting in each component adsorption. [$SnO_2$ nano-object dewet/PDDA/PSS] were done by 10 s dipping followed by dewetting of the $SnO_2$ dispersion in 50% DMF.

**Acknowledgment.** J.L. gratefully acknowledges the support of the Ministry of Information & Communications, Republic of Korea, under the Information Technology Research Center (ITRC) Support Program.

**Supporting Information Available:** Young's equation analysis; SEM image of branched nanowires from $SnO_2$. This material is available free of charge via the Internet at http://pubs.acs.org.

## References

(1) Decher, G. *Science* **1997**, *277*, 1232.
(2) Hammond, P. T. *Adv. Mater.* **2004**, *16*, 1271.
(3) Mamedov, A.; Ostrander, J. W.; Aliev, F.; Kotov, N. A. *Langmuir* **2000**, *16*, 3941−3949.
(4) Kovtyukhova, N. I.; Mallouk, T. E. *J. Phys. Chem. B* **2005**, *109*, 2540.
(5) Wu, Z.; Walish, J.; Nolte, A.; Zhai, L.; Cohen, R. E.; Rubner, M. F. *Adv. Mater.* **2006**, *18*, 2699.
(6) Schlenoff, J. B.; Dubas, S. T.; Farhat, T. *Langmuir* **2000**, *16*, 9968.
(7) Izquierdo, A.; Ono, S. S.; Voegel, J.-C.; Schaaf, P.; Decher, G. *Langmuir* **2005**, *21*, 7558.
(8) Jiang, C.; Markutsya, S.; Tsukruk, V. V. *Langmuir* **2004**, *20*, 882.
(9) Lee, S. S.; Hong, J.-D.; Kim, C. H.; Kim, K.; Koo, J. P.; Lee, K.-B. *Macromolecules* **2001**, *34*, 5358.
(10) Cho, J.; Char, K.; Hong, J.-D.; Lee, K.-B. *Adv. Mater.* **2001**, *13*, 1076.
(11) Chiarelli, P. A.; Johal, M. S.; Casson, J. L.; Roberts, J. B.; Robinson, J. M.; Wang, H.-L. *Adv. Mater.* **2001**, *13*, 1167.
(12) Sun, J.; Gao, M.; Feldmann, J. *J. Nanosci. Nanotechnol.* **2001**, *1*, 133.
(13) Fujimoto, K.; Fujita, S.; Ding, B.; Shiratori, S. *Jpn. J. Appl. Phys.* **2005**, *44*, L126−L128.
(14) Picart, C.; Mutterer, J.; Richert, L.; Luo, Y.; Prestwich, G. D.; Schaaf, P.; Voegel, J.-C.; Lavalle, P. *Proc. Natl. Acad. Sci. U.S.A.* **2002**, *99*, 12531.
(15) Nam, K. T.; Kim, D.-W.; Yoo, P. J.; Chiang, C.-Y.; Meethong, N.; Hammond, P. T.; Chiang, Y.-M.; Belcher, A. M. *Science* **2006**, *312*, 885.
(16) Maheshwari, V.; Saraf, R. F. *Science* **2006**, *312*, 1501.
(17) Ko, H.; Jiang, C.; Shulha, H.; Tsukruk, V. V. *Chem. Mater.* **2005**, *17*, 2490.
(18) Mamedov, A. A.; Kotov, N. A.; Prato, M.; Guldi, D. M.; Wicksted, J. P.; Hirsch, A. *Nat. Mater.* **2002**, *1*, 190.
(19) Olek, M.; Ostrander, J.; Jurga, S.; Mohwald, H.; Kotov, N.; Kempa, K.; Girsig, M. *Nano Lett.* **2004**, *4*, 1889.
(20) Shim, B. S.; Starkovich, J.; Kotov, N. *Compos. Sci. Technol.* **2006**, *66*, 1174.
(21) Wang, Y.; Tang, Z.; Podsiadlo, P.; Elkasabi, Y.; Lahann, J.; Kotov, N. A. *Adv. Mater.* **2006**, *18*, 518.
(22) Podsiadlo, P.; Choi, S.-Y.; Shim, B.; Lee, J.; Cuddihy, M.; Kotov, N. A. *Biomacromolecules* **2005**, *6*, 2914.
(23) Correa-Duarte, M. A.; Kosiorek, A.; Kandulski, W.; Giersig, M.; Salgueinño-Maceira, V. *Small* **2006**, *2*, 220.
(24) Rouse, J. H.; Lillhei, P. T.; Sanderson, J.; Siochi, E. J. *Chem. Mater.* **2004**, *16*, 3904.
(25) Rouse, J. H.; Lillehei, P. T. *Nano Lett.* **2003**, *3*, 59.
(26) Correa-Duarte, M. A.; Kosiorek, A.; Kandulski, W.; Giersig, M.; Liz-Marzan, L. M. *Chem. Mater.* **2005**, *17*, 3268.
(27) Sato, M.; Sano, M. *Langmuir* **2005**, *21*, 11490.
(28) Paloniemi, H.; Lukkarinen, M.; Aaritalo, T.; Areva, S.; Leiro, J.; Heinonen, M.; Happakka, K.; Lukkari, J. *Langmuir* **2006**, *22*, 74.
(29) Kong, H.; Luo, P.; Gao, C.; Yan, D. *Polymer* **2005**, *46*, 2472.
(30) Reiter, G. *Phys. Rev. Lett.* **1992**, *68*, 75.
(31) Reiter, G.; Levent Demirel, A.; Granick, S. *Science* **1994**, *263*, 1741.
(32) Lu, N.; Chen, X.; Molenda, D.; Naber, A.; Fuchs, H.; Talapin, D. V.; Weller, H.; Muller, J.; Lupton, J. M.; Feldmann, J.; Rogach, A. L.; Chi, L. *Nano Lett.* **2004**, *4*, 885.
(33) Huang, J.; Kim, F.; Tao, A. R.; Connor, S.; Yang, P. D. *Nat. Mater.* **2005**, *4*, 896.
(34) Cebeci, F. C.; Wu, Z.; Zhai, L.; Cohen, R. E.; Rubner, M. F. *Langmuir* **2006**, *22*, 2856.
(35) Serizawa, T.; Kamimura, S.; Kawanishi, N.; Akashi, M. *Langmuir* **2002**, *18*, 8381.
(36) Blossey, R. *Nat. Mater.* **2003**, *2*, 301.
(37) Shim, B. S.; Kotov, N. A. *Langmuir* **2005**, *21*, 9381.
(38) Tang, Z.; Wang, Y.; Kotov, N. A. *Langmuir* **2002**, *18*, 7035.
(39) Reiter, G.; Sharma, A. *Phys. Rev. Lett.* **2001**, *87*, 166103−166103/4.
(40) Yerushalmi-Rozen, R.; Kerle, T.; Klein, J. *Science* **1999**, *285*, 1254.
(41) Sinani, V. A.; Gheith, M. K.; Yaroslavov, A. A.; Rakhnyanskaya, A. A.; Sun, K.; Mamedov, A. A.; Wicksted, J. P.; Kotov, N. A. *J. Am. Chem. Soc.* **2005**, *127*, 3463.
(42) Thiele, U.; Mertig, M.; Pompe, W. *Phys. Rev. Lett.* **1998**, *80*, 2869.
(43) Ghatak, A.; Khanna, R.; Sharma, A. *J. Colloid Interface Sci.* **1999**, *212*, 483.
(44) Deegan, R. D.; Bakajin, O.; Dupoint, T. F.; Huber, G.; Nagel, S. R.; Witten, T. A. *Nature* **1997**, *389*, 827.
(45) Gaponik, N.; Talapin, D. V.; Rogach, A. L.; Hoppe, K.; Shevchenko, E. V.; Kornowski, A.; Eychmuller, A.; Weller, H. *J. Phys. Chem. B* **2002**, *106*, 7177.
(46) Tang, Z.; Kotov, N. A.; Giersig, M. *Science* **2002**, *297*, 237.
(47) Herminghaus, S. *J. Phys.: Condens. Matter* **2005**, *17*, S261−S263.
(48) Javey, A.; Nam, S. W.; Friedman, R. S.; Yan, H.; Lieber, C. M. *Nano Lett.* **2007**, *7*, 773−777.

NL071245D